146. D. Shopov and A. Andreev, *Kinet. Katal.*, 28, (1987), 133.

147. M.I. Temkin, *Adv. Catal.*, 28, (1979), 263.

148. P.C. Ford, *Acc. Chem. Res.*, 14, (1981), 31.

149. M.I. Temkin and N.V. Kul'kova, *Zh. Fiz. Chim.*, 23, (1949), 695.

150. G.K. Boreskov, T.M. Yur'eva and A.S. Sergeeva, *Kinet. Katal.*, 11, (1970), 1476.

151. T. van Herwijnen and W.A. de Jong, *J. Catal.*, 63, (1980), 83.

152. G.C. Chinchen, M.S. Spencer, K.C. Waugh, and D.A. Wahn, *J. Chem. Soc., Faraday Trans. 1*, 83, (1987), 2193.

153. G.C. Chinchen, K. Mansfield and M.S. Spencer, *Chemtech*, Nov. 1990.

154. T.M. Yur'eva, G.K. Boreskov and V. Sh. Gruver, *Kinet. Katal.*, 10, (1969), 862.

155. M.A. Vannice, *J. Catal.*, 50, (1977), 228.

156. E.F. Armstrong and T.P. Hilditch, *Proc. Roy. Soc. Ser.*, A97, (1920), 265.

157. T. Shido, K. Asakura and Y. Iwasawa, *J. Catal.*, 122, (1990), 55.

158. T. Shido and Y. Iwasawa, *J. Catal.*, 129, (1991), 343.

159. I. T. Horvath and M. Siskin, *Energy Fuels*, 5, (1991), 932.

160. E. Calbourn, R.A. Hadden, H.D. Vandervell, K.C. Waugh, and G. Webb, *J.Catal.*, 130, (1991), 514.

161. T. Salmi and R. Hakkarainen, *Appl. Catal.*, 49, (1989), 285.

162. G.J. Hutchings, F.M. Gottschalk, R. Hunter and S.W. Orchard, *J. Chem. Soc., Faraday Trans. I*, 85, (1989), 363.

163. D.C. Elliot, R.T. Hallen and L.J. Sealockjr, *Ind. Eng. Chem., Prod. Res. Dev.*, 22, (1983), 431.

164. H. Bohlbro, "*An Investigation on the Kinetics of the Conversion of Carbon Monoxide with Water Vapour over Iron Oxide Based Catalysts*", 2nd. Ed., Gjellerup, Copenhagen, (1969).

165. J.M. Moe, *Chem. Eng. Prog.*, 58, (1962), 33.

166. M.I. Temkin, N.M Morozov and G.G. Shibrya, *Kinet. Katal.*, 6, (1965), 1057.

167. W.F. Podolski and Y.G. Kim, *Ind. Eng. Chem. Process, Des. Dev.*, 13, (1974), 415.

168. M. Boudart, *A.I.Ch.E. J.* 2, (1956), 62.

169. P. Hou, D. Meeker and H. Wise, *J. Catal.*, 80, (1983), 280.

CHAPTER TWO

EXPERIMENTAL

2.1 CATALYST PREPARATION

2.1.1 Alloy catalysts

(a) Alloy preparation

The alloys Cu-Aℓ and Cu-Zn-Aℓ were prepared by Matex (Pty) Limited South Africa, using high purity metals (conductivity grade copper > 99% purity, zinc thermal spray wire > 99.8% purity and aluminium thermal spray wire > 99.5% purity) melted in an AC50 silicon carbide crucible, using a gas fired furnace.

Two methods of preparation were adopted. The Cu-Aℓ binary alloy was prepared by first melting the required amount of copper (M.P. = 1083°C) and then adding the required aluminium (M.P. = 660°C). The alloy melt was stirred thoroughly with a green pole and rapidly quenched by pouring into agitated cold water. In some cases, a similar procedure was adopted to prepare the Cu-Zn-Aℓ ternary alloys. A Cu-Aℓ melt was made as described above, and cooled to *below* 420°C (melting point of zinc) before the required amount of zinc was added to the melt. This procedure helped to prevent rapid vaporisation of the lower melting zinc metal. Rapid stirring and cold water quenching of the melt completed the process.

The second method involved the preliminary formation of Aℓ-Zn and Aℓ-Cu precursor alloys, which, taken in required proportions were melted together, vigorously stirred and rapidly quenched in cold water. This method was preferred for the preparation of ternary alloys as it ensured greater homogeneity through more thorough mixing of metal components.

Oxidation was prevented by the gas combustion products and an artificial nitrogen blanket inserted under the furnace hood.

The alloy product, in the form of prills ± 50 mm x 5 mm were crushed using a Christie-Norris hammer mill and screened to provide a product range up to 2 mm in diameter. Batch sizes between 500 and 800 g were prepared.

The nominal and atomic absorption (see Section 2.5.1) analysed bulk composition of the five alloys prepared for this study are represented in Table 2.1.

Table 2.1 Alloy bulk composition

Alloy	Alloy Compositions (wt%) *					
	Nominal			Analysis		
	Cu	Zn	Al	Cu	Zn	Al
A	10	40	50	13.4	34.0	51.0
B	25	25	50	24.8	25.2	48.3
C	35	15	50	40.4	11.3	47.7
D	50	0	50	52.3	0	48.0
E	43	18	39	41.7	20.5	37.5

* Error: ± 2.0 wt% (see Section 2.5.1)

Alloys A-D were chosen with 50 nominal wt% aluminium and varying amounts of copper and zinc. The 50 wt% aluminium yields an alloy which corresponds to a product which contains a maximum amount of the primary precipitate $CuAl_2$, reported (1) to be the leachable phase that produces Raney copper. Alloy E was included because some authors (2, 3) observed that catalysts prepared from these alloys had both greater methanol synthesis activity and greater mechanical strength than those prepared from alloys with higher Al contents. The nominal alloy compositions are shown plotted on the Al-Cu-Zn liquidus projection diagram in Figure 2.1.

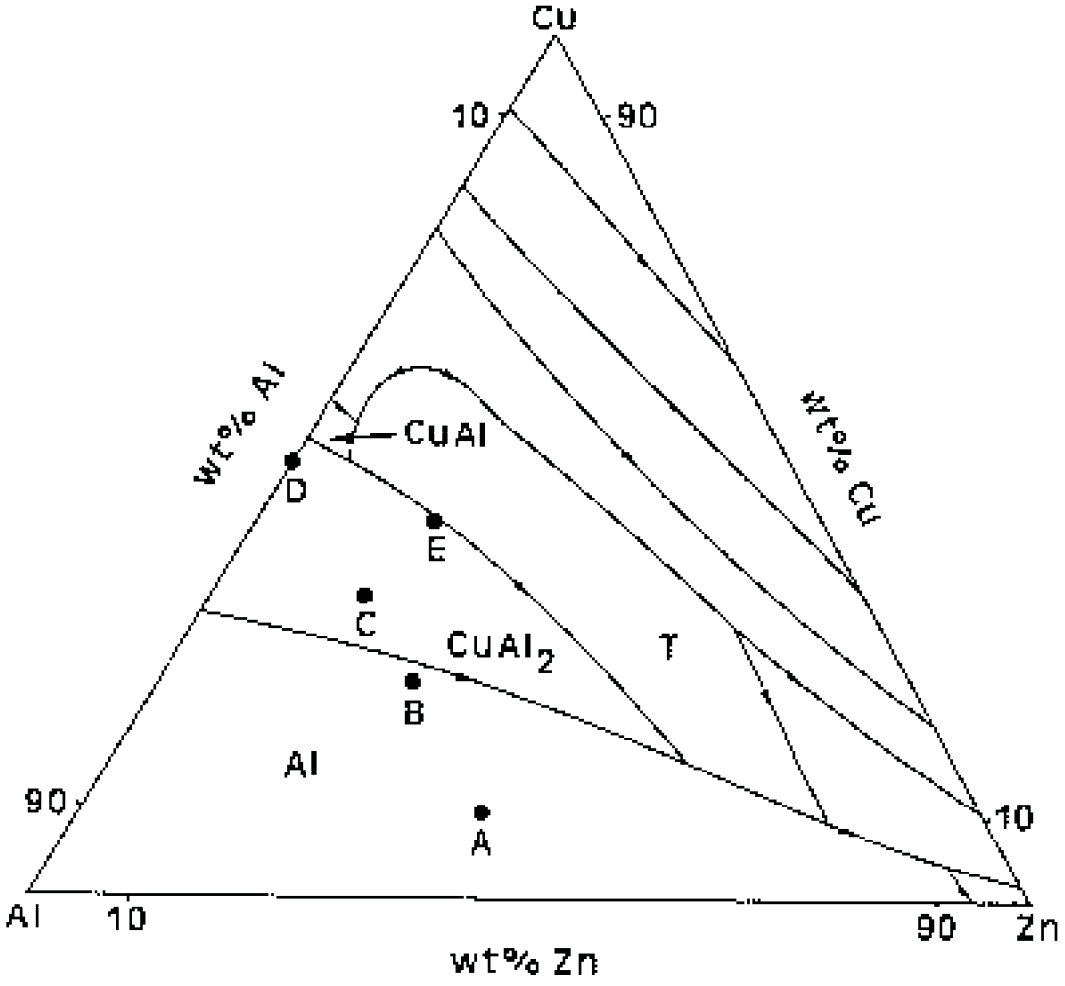

T = ternary phase

Figure 2.1 The liquidus projection (1, 4) for the Cu-Zn-Al system showing the compositions of the nominal alloys (●) and specific phase regions of interest

(b) Caustic leaching

Raney copper catalysts were prepared from the alloys by a procedure similar to that adopted by Marsden *et al.* (5), unless otherwise stated. In these experiments 20 g of alloy particles 0.50 to 1.180 mm in diameter were placed in 111 g of de-ionized water, contained in an open necked 500 ml round-bottomed flask, suspended in a constant temperature water bath at 50°C. After the solution reached temperature equilibrium, 111ml of 14.1 M aqueous sodium hydroxide solution was added dropwise over one hour to achieve a final leach concentration of 7.06 M. The amount of caustic solution provided was equivalent to more than four times

the stoichiometric amount of aluminium present in the alloy. No means of stirring was provided as it could lead to the uneven mechanical breakdown of the catalyst porous reaction rim. The reaction temperature was controlled at 50 ± 3.5°C. The extent of the reaction was determined by the time of contact of alloy in the caustic solution. After extraction had taken place to the desired conversion, the catalyst particles were thoroughly washed with de-ionized water until the pH of the wash water was 7. The Raney copper catalyst was then allowed to rapidly oxidise by drying in air at 120°C for one hour, or was passivated by exposure to nitrous oxide. Passivation comprises the mild reversible oxidation of the exposed copper surface, using a technique described in Appendix 1.

The chemical reactions involved in the leaching of the Cu-Zn-Aℓ alloys with caustic solution (5) may be represented as follows:

$$Al + OH^- + 3H_2O \rightarrow Al(OH)_4^- + 3/2H_2 \qquad - (2.1)$$

$$Zn + 2OH + 2H_2O \rightarrow Zn(OH)_4^{2-} + H_2 \qquad - (2.2)$$

Prior to reactor testing, all passivated and air dried Raney catalysts were re-sieved in order to remove small copper fines generated during the leach reaction. No formal calcination procedure was necessary.

(c) Acid leaching

In this case, 10.00 g batches of ternary Cu-Zn-Aℓ alloys of diameter 0.50 to 1.180 mm were leached in final solutions of either nitric or perchloric acid of 5%, 14% or 27.5% strength, using an almost identical procedure already outlined for base leaching. Acid solution corresponding to three times the stoichiometric amount of aluminium was added dropwise over 15 minutes to an equal volume of de-ionized water containing the alloy particles. Following

the leach reaction at 50 ± 3.5°C, the catalyst particles were removed from the acid environment and thoroughly washed with de-ionized water until the pH of the wash water was 7. Raney copper catalyst preparation was completed by air drying at 120°C for one hour. Unlike with caustic leached alloys, it is impossible to present the precise stoichiometry of chemical reactions occurring due to the complexity of alloy reaction with nitric and perchloric acid. The following reaction equations are therefore assumptions:

(i) **Nitric acid leached alloys:**

$$Cu\text{-}Zn\text{-}Al + HNO_3(conc.) \rightarrow Cu(NO_3)_2 + NO_2 \quad - (2.3)$$

$$Cu\text{-}Zn\text{-}Al + HNO_3(dil.) \rightarrow Cu(s) + Al^{3+} + Zn^{2+} \quad - (2.4)$$

The concentrated nitric acid (Equation 2.3) acts as an oxidising agent.

(ii) **Perchloric acid leached alloys:**

$$Cu\text{-}Zn\text{-}Al + HClO_4 \rightarrow Cu(s) + Al^{3+} + Zn^{2+} \quad - (2.5)$$

The validity of these assumptions are discussed in Chapter 4.

(d) <u>Alkali promoted Raney copper catalysts</u>

The optimised Raney Cu-Zn-Al catalyst (see Chapter 6) was modified by promotion with alkali metal, using a process developed by Klier *et al.* (6) for similar promotion of co-precipitated Cu-ZnO methanol synthesis/WGS catalysts. This process was utilised to promote the optimised Raney copper catalyst with 0.1, 0.5 or 1.0 nominal mol% levels of either cesium, rubidium or potassium. Thus, a total of nine promoted catalysts were prepared for reactor testing.

Typically, 3.000g of Raney catalyst was added to 25ml of aqueous solution containing the calculated mass of alkali metal (CsOH, RbOH or KOH) required for promotion. The solution contained in a 75ml glass beaker was slowly evaporated to dryness in a constant temperature water bath controlled at 50 ± 3.5°C.

(e) Zinc implanted Raney copper catalysts

Catalysts were prepared for ion implantation as follows: Alloy particles of diameter 1.000 to 1.180mm with a nominal composition of 50wt% Cu and 50wt% Aℓ - Cu(50)Aℓ(50) - were passivated after leaching in 5.3M NaOH for one hour in accordance with the procedure outlined in Appendix 1.

Batches of 3.000g of Raney catalyst were implanted according to the detailed description outlined in Appendix 2 for a dosage time that is related to the total ion dosage level required by the following relationship:

$$T = \frac{D \times A \times q}{I \times 60} \qquad \text{- (2.6)}$$

where: T = dosage time (minutes)
D = ion dosage (ions.cm^{-2})
A = total surface area of target material (cm^2)
q = charge of electron (1.602×10^{-19}C)
I = operating current (A)

Spherical particles were assumed for the calculation of total surface area (A).

2.1.2 Co-precipitation

The preparation of catalysts by co-precipitation of the constituent metal salts under controlled reaction conditions (temperature, pH and reagent flow rate), usually produces a reproducible homogeneous mixing of the respective metal ions (7).

The procedure of preparation of co-precipitated cobalt-manganese and cobalt-chromium catalysts was developed by co-workers (8) after consideration of several variations on the method outlined by Maiti et al. (9). Nitrate metal salts were precipitated from an ammoniacal solution. Sulphate and chloride salts, which are known catalyst poisons (Chapter 1) were avoided. A small scale laboratory set-up resulted in a modest recovery of reagents (± 10 g per batch) as outlined in Appendix 3. Larger amounts (± 100 g) of catalyst were prepared at the Chemical Engineering Department, University of Potchefstroom, Vaal Campus (South Africa) by a continuous co-precipitation method, described by Deckwer et al. (10).

A co-precipitated copper-zinc-aluminium low temperature CO-shift catalyst was prepared at ENERTEK, CSIR, Pretoria, South Africa, using a procedure outlined by Stiles (11) and reported in Appendix 3. A ratio of two zinc to one copper (by mass) resulted in a catalyst of required formulation that is generally preferred (11) by plant operators.

2.1.3 Catalyst pelleting and calcination

After calcination, the fine powdered catalyst precursors were pressed into non uniform discs of ± 2 mm thickness between two sheets of wax paper using a portable hydraulic press (20 tons.cm^{-2}). The discs were broken down and sieved to obtain a particle size distribution from 0.500 to 1.180 mm. The particles were then loaded into a muffle furnace and the Co-based material calcined in air at 500°C for 24 hours, whilst the Cu based material was also calcined in air at 300°C for 7 hours.

2.1.4 Analysis of metal content

The bulk metal composition of alloy and co-precipitated catalysts was determined by atomic absorption spectroscopy. Details of the procedures used are given in Section 2.5.

2.2 CATALYST TESTING

2.2.1 Pretreatment and start-up procedures

Catalyst batches of 2 ± 0.1ml were loaded into fixed-bed laboratory microreactors (detailed in Section 2.2.2) and reduced *in situ* under H_2.

Alloy and co-precipitated Cu-based catalysts were reduced according to a procedure similar to that described for the ICI 53-1 low temperature shift catalyst (12) which is outlined below:

Following a reactor purge to remove oxygen, the catalyst was heated in inert N_2 (99.999% purity) to 120°C at a rate of 50°C/hour. A premixed 5% H_2/N_2 (by vol.) gas was substituted at a GHSV = 900 h^{-1} and reduction commenced. The catalyst temperature was increased to a maximum of 230°C (ideally 30°C/hour) and maintained for 16 hours. At all stages of reduction, care was taken to prevent exothermic temperature run-aways.

Co-precipitated Co-based catalysts were reduced isothermally in a pure H_2 (GHSV = 200 h^{-1}) stream at 400°C for 16 hours.

After reduction, the catalysts were cooled to 200°C and the reactor flushed with nitrogen prior to the introduction of reagent gases.

2.2.2 Microreactor systems

Low temperature Cu-based WGS catalysts were tested for activity and stability using two banks of three fixed-bed, stainless steel laboratory microreactors, as illustrated in Figure 2.2. Sulphur co-feed experiments were conducted in an isolated bank of two fixed-bed laboratory microreactors, housed in a fume-hood. A schematic diagram is given in Figure 2.3.

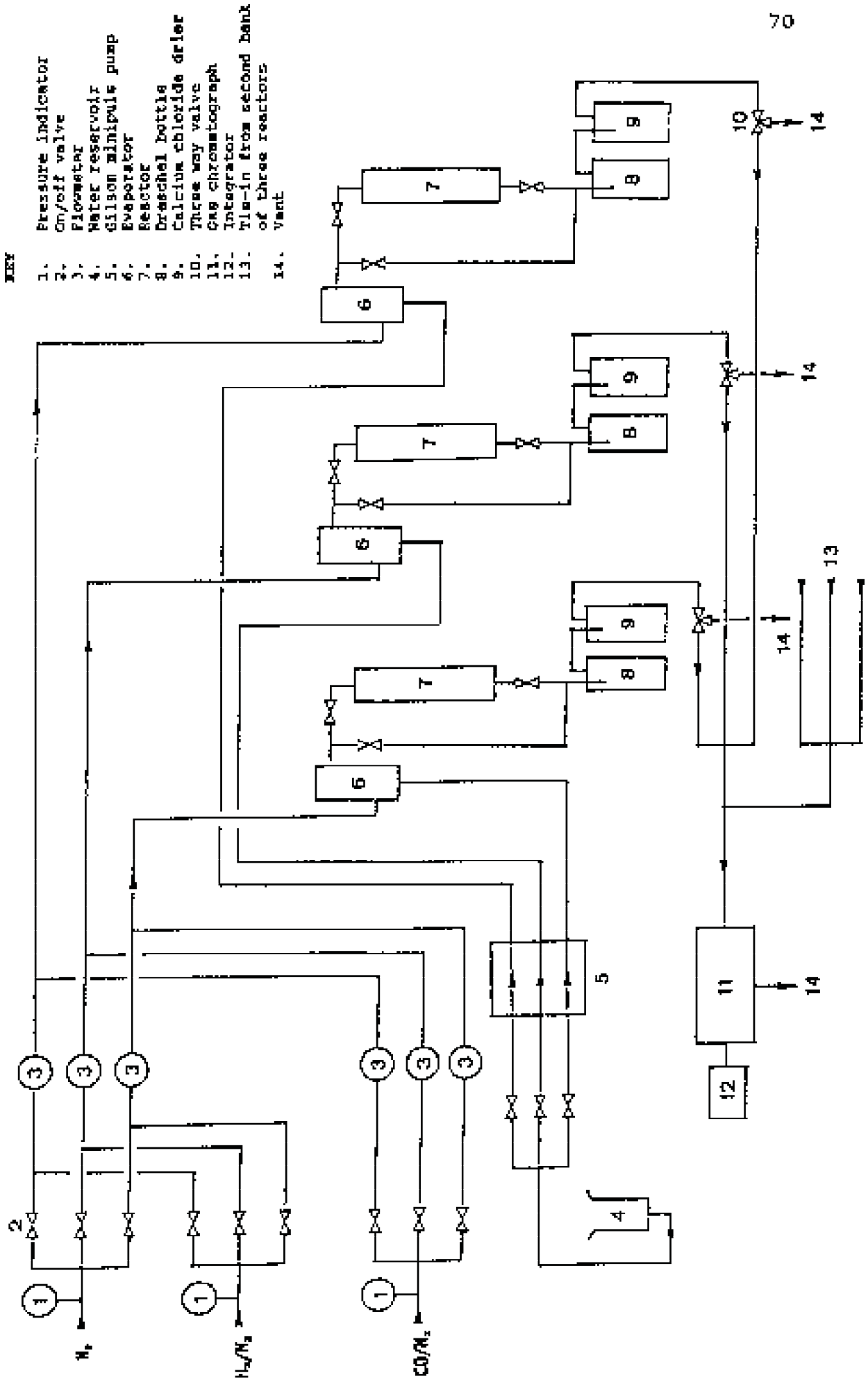

Figure 2.2 Schematic representation of one bank of three reactors for evaluating copper-based catalysts

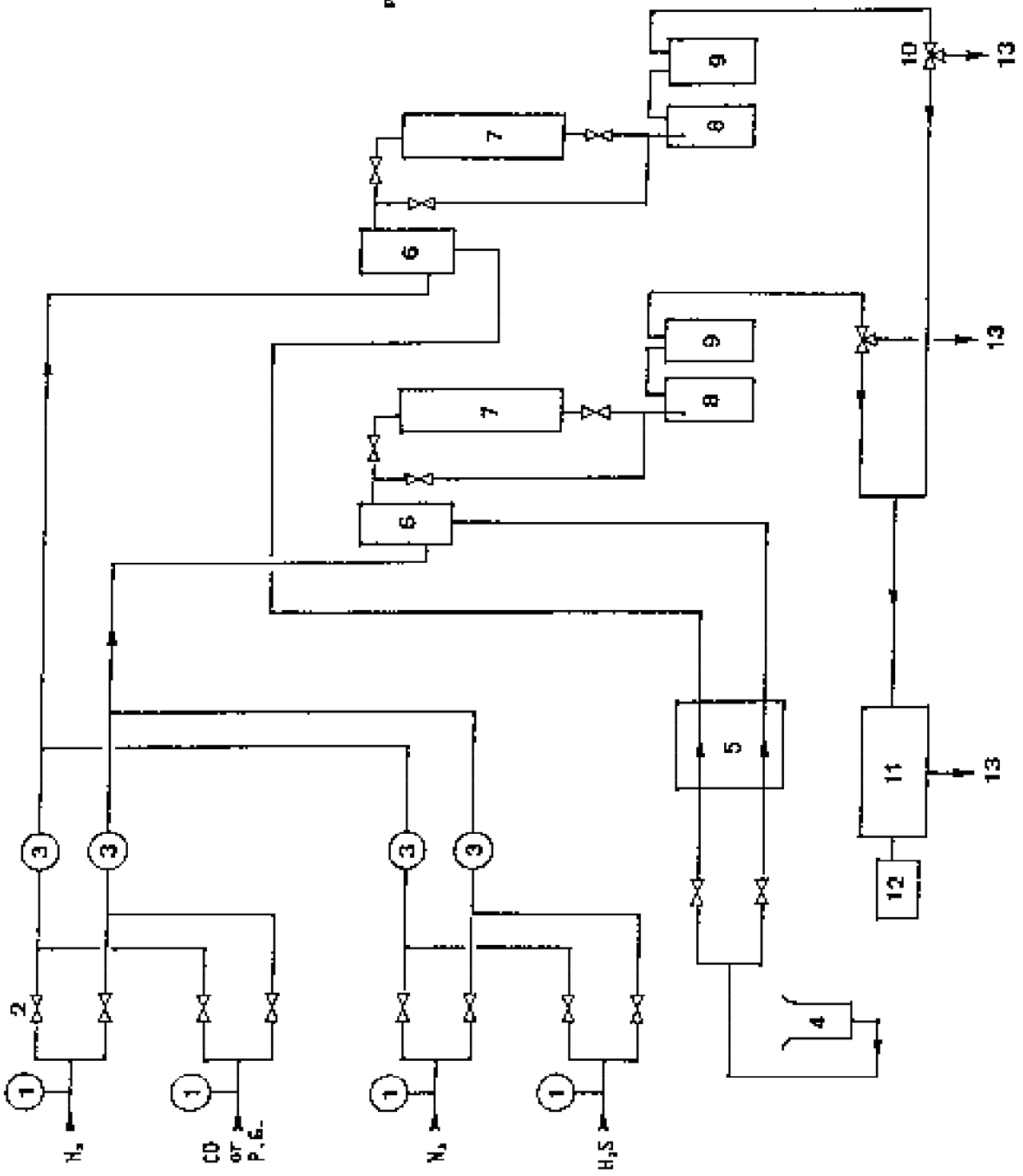

Figure 2.3 Schematic representation of the catalyst testing apparatus for sulphur co-feed experiments

Both reactor assemblies enabled independent catalytic testing under approximately identical experimental conditions. Construction was from 1/4" stainless steel tubing and stainless steel Swagelock connections (Johannesburg Valve and Fitting, South Africa).

Carbon monoxide and nitrogen (introduced as an inert tracer gas and catalyst coolant) of > 99.9% purity (supplied by Afrox, South Africa) or a premixed gas (typically 10% CO/N_2 (by vol.) supplied by Fedgas, South Africa) and other reagent gases e.g. hydrogen (for reduction), were fed to the evaporators of the respective reactor assemblies. Flow rates were controlled using Whitey fine control needle valves, situated upstream from the respective flow indicators (0 - 2 l gas/hour Aalburg Instruments and Control Inc. USA). De-ionized water from the reservoir was pumped into the evaporators (Appendix 4) by means of a Gilson Minipuls peristaltic pump. The evaporators were maintained at 130°C using thermostatically controlled electric heating tape (supplied by Electric Elements, South Africa). To prevent water condensation, the outlet line of the evaporator to the inlet of the microreactor was heated between 120°C and 150°C using electric heating tapes regulated by J-type thermocouples and thyristor controllers.

Two types of reactor design and heating methods were used. Modified Helico flex sealed Korf and Espinoza (13) reactors (Type 1, detailed in Appendix 4) were heated by means of electric heating tapes as described for line temperature control. Modified type 1 vacuum sealed Korf and Espinoza (13) reactors (Type 2, detailed in Appendix 4) were heated by means of electronic heating jackets (Heating Element Engineering, South Africa) and the temperature regulated by K-type thermocouples and thyristor controllers. (RKC Instruments). The sulphur co-feed experimental reactors and one bank of three low temperature WGS reactors were configured in this design, (Type 2) whilst the remaining bank of three were configured in the former design (Type

1). In both cases, an additional thermocouple was inserted into the catalyst bed for accurate temperature measurements during the reaction. For all data quoted, temperature control was better than ± 1.0°C.

A dual-trap system removed unreacted water from the product gas mixture before analysis. This was necessary as water could have damaged the gas chromatographic columns. The trap system consisted of two 500ml Dreschel bottles per reactor. Water condensed in the first trap and was completely removed in the second which contained anhydrous calcium chloride drying agent. Both traps were kept at room temperature.

The mechanistic co-feeding experiments were carried out in a glass micro-reactor. The glass reactor assembly also allowed for the introduction of organic liquids by controlled evaporation as detailed in Appendix 5.

2.3 PRODUCT ANALYSIS

2.3.1 Gas analysis from the reactor-assembly testing Cu-based catalysts

Gaseous products from the reactors were fed into three-way solenoid valves (ASCO, USA) which enabled the analysis of product gases from a *selected* reactor by the on line thermal conductivity detector (TCD) of a Hewlett Packard 5730A gas-solid chromatograph. A pneumatically operated six port sample valve (Valco) was used to inject the product gas from a 1ml sample loop into a 3m x 1/8" stainless steel Carbosphere column (Alltech Associates, 60-80 mesh) operated isothermally at 60°C (using Ar as a carrier gas). Separation was adequate for the fixed gases i.e. H_2, N_2, CO, CH_4 and CO_2, although separation of N_2 and O_2 could *not* be achieved with this column. However, periodic separate off-line analyses, using a molecular sieve column confirmed that O_2 levels of less than 0.001% mol. were present in product gases.

An on-line Spectra-Physics 4290 electronic integrator equipped with an external events module was used to fully automate the continuous selective gas sampling of each reactor in the multi-reactor systems. Gaseous hydrocarbons (C_1-C_{12}) were analysed using a temperature programmed 2 m x 1/8" stainless steel Porapak Q column (Waters Associates Inc., 80 - 100 mesh) and the flame ionisation detector (FID) of an off-line Pye Unicam 204 gas chromatograph (using N_2 as a carrier gas). A manually operated six port sample valve (Valco) was used to inject gas mixtures from a 1 ml sample loop into the column.

2.3.2 Analysis of gas from the sulphur co-feeding reactor assembly

A similar three-way solenoid valve set-up enabled either of the reactor gas streams to be channelled into the 0.25 ml sample loop of an on-line Hewlett Packard 5890A (Flame Photometric Detector - FPD) gas chromatograph. A pneumatically operated six port sample valve (Valco) injected the selected gas sample into a Chromosil 310, 2 m x 4 mm ID glass column, isothermal at 60°C. Good separation of COS, H_2S, CS_2 and SO_2 was observed in the N_2 carrier gas (20 ml/min).

Simultaneous TCD analysis of the fixed gas i.e. H_2, N_2, CO, CH_4 and CO_2 was achieved using a gas chromatograph built for the application (Wits University). Detector and oven temperature were regulated isothermally at 180°C and 100°C respectively, using proportional integral derivative (PID) control. Once again, a pneumatically operated six port sample valve facilitated accurate injection of a 1 ml gas sample into the 2 m x 1/8" stainless steel Carbosieve SII column (Supelco, USA 60 - 80 mesh). He (99.999% purity) carrier gas was used (25 ml/min).

2.4 DATA EVALUATION

All gas chromatographic data obtained was analysed by the built-in data evaluation programs of a Spectraphysics SP4290 electronic integrator. These programs were routinely used to obtain quantitative product analyses. A detailed description is given in Appendix 6.

2.5 CATALYST CHARACTERISATION

2.5.1 Bulk characterisation

(a) Atomic Absorption Spectroscopy

The bulk metal composition of all catalysts was determined by atomic absorption spectroscopy (Varian Techtron AA4). Cobalt manganese oxide and cobalt chromium catalysts were analysed using the standard addition method. Samples of 0.100 g of these catalysts were dissolved in minimum aqua regia (± 10 ml, boiling for 5 minutes) and diluted up to 1 l with distilled water. The molar concentration of the metal components was then determined using standard solutions as calibrants.

Alloys and catalysts containing Cu, Zn and Al were analysed by exactly matching the composition of standard and sample solutions according to the procedure outlined in Appendix 7. Error of determination was ± 2 wt%.

(b) Inductively Coupled Plasma-Mass Spectroscopy (ICP-MS)

The alkali metal and ion implanted zinc content of Raney copper catalysts was determined at MINTEK (Randburg, South Africa) using ICP-MS. Standards were matched to samples using the method outlined in Appendix 7 to avoid possible chemical interference effects. All concentration levels analysed for, were well within the detection limits of this technique.

(c) X-Ray Diffraction analysis (XRD)

A Phillips PW 1050 diffractometer (incorporating a copper anode and graphite monochromator) was used to determine the crystalline bulk structure of alloys, catalysts and catalyst precursors. The identification of XRD patterns was either manually determined using data in the JCPD file or aided by computer controlled peak search routines.

(d) Thermal analysis

Differential Scanning Calorimetry and Thermal Gravimetric Analysis was carried out using a Dupont 9900 thermal analysis system linked to a 910 DSC and 951 TGA module. The thermal analyses were performed under selected atmospheres by use of a gas manifold system. Gas flow rates were typically 30 ml/min, which ensured continued adequate flushing of the TGA and DSC cells.

2.5.2 Surface characterisation

(a) Scanning Electron Microscopy (SEM)

SEM measurements were performed at AECI (Modderfontein, South Africa) using a JEOL JSM-35CF Scanning Microscope with EDAX and elemental mapping facilities. EDAX error of determination was 2 - 5 wt%.

(b) Surface area measurements

Specific copper surface areas were determined by nitrous oxide pulse experiments based on the procedure reported by Evans *et al.* (14). A detailed description of the technique and instrument is presented in Chapter 3.

Active copper metal dispersion is expressed in terms of the ratio of the total number of surface atoms to the total number of metal atoms present, according to Equation 2.7.

$$D_M = N(S)_M / N(T)_M \qquad - (2.7)$$

where: D_M = active metal (M) dispersion (%)
$N(s)M$ = number of moles (surface)
$N(T)M$ = number of moles (total)

Copper particle volume-area mean diameter (d_{VA}) was calculated from the expression (15) based on the spherical equivalent approximation:

$$\bar{d}_{VA} = 6\left(\frac{V_M}{a_M}\right) / D_M \qquad - (2.8)$$

where: a_M = effective average area occupied by a metal atom in the surface
V_M = volume per metal atom in the bulk
D_M = active metal (M) dispersion (%)

BET surface area measurements were determined using a Carlo Erba Sorptomatic Series 1800 analyser. Pore size distributions were determined from the Kelvin Equation using data obtained from the desorption isotherm (16). *In situ* BET surface areas were determined using the copper surface area analyser detailed in Chapter 3.

(c) Fourier Transform-Infra Red Spectroscopy (FT-IR)

A Bruker IFS 85 Spectrometer with a Diffuse Reflectance Optical accessory (Marrick) was used to determine reaction intermediates in an *in situ* Reaction Chamber (Marrick).

(d) X-Ray Photoelectron Spectroscopy (XPS)

In-situ XPS was used to determine the nature of sulphur adsorption onto two cobalt based high temperature WGS

catalysts (see Chapter 8). Experiments were conducted in a Vacuum Generator "Solar 300" chamber (base pressure 4×10^{-10} bar) with a VG 'CLAM 100' system comprising of a standard (Mg/Al) water cooled anode and a LEG61 electron gun, mounted in the chamber. These sources shared a 150° spherical detector analyser and a channeltron detector. The catalyst reactor consisted of a Leybold-Heraeus VLP10/63 preparation chamber which was connected to a high pressure cell which was in turn linked to the UHV chamber. The catalyst disc was mounted on a molybdenum sample holder which fitted into a recess in a motor driven cylindrical rod. The sample was heated resistively by passing a current through the sample holder.

2.6 LITERATURE

1. J.B. Friedrich, D.J. Young and M.S. Wainwright, *J. Electrochem. Soc.*, 128, (1981), 1840.

2. M.S. Wainwright, in "*Methane Conversion*", Elsevier Science Publishers B.V., Amsterdam, (1988), 95.

3. H.E. Curry-Hyde, M.S. Wainwright and D.J. Young, *Appl. Catal.*, 77, (1991), 89.

4. L.F. Mondolfo, "*Aluminium Alloys: Structures and Properties*", Butterworths, London, (1976).

5. J.B. Friedrich, D.J. Young and M.S. Wainwright, *J. Electrochem. Soc.*, 128, (1981), 1845.

6. K. Klier, C-W Young and J.G. Nunan, *Ind. Eng. Chem. Fundam.*, 25, (1986), 36.

7. G.J.K. Acres, A.J. Bird, J.W. Jenkins and F. King, in "*Catalysis Specialist Periodical Reports - Vol. 4*", The Royal Society of Chemistry, London, (1981), Chap. 1.

8. M. van der Riet, *PhD Thesis*, University of the Witwatersrand, Johannesburg, South Africa, (1988).

9. G.C. Maiti, R. Malessa and M. Baerns, *Appl. Catal.*, 5, (1983), 151.

10. W.D. Deckwer, Y. Serpemen, M. Ralek and B. Schmidt, *Ind. Eng. Chem. Process Des. Dev.*, 21, (1982), 222.

11. A.B. Stiles, *"Catalyst Manufacture Laboratory and Commercial Preparations"*, Marcel Dekker Inc., New York and Basel, (1983), 118.

12. *"ICI Catalysts Operating Manual"*, Imperial Chemical Industries, Billingham, Cleveland, England, (1986).

13. C.J. Korf and R. Espinoza, *CSIR (CENG) Report*, Pretoria, South Africa, (1986), 584.

14. J.W. Evans, M.S. Wainwright, A.J. Bridgewater and D.J. Young, *Appl. Catal.*, 7, (1983), 75.

15. J.R. Anderson and K.C. Pratt, *"Introduction to Characterisation and Testing of Catalysts"*, Academic Press Inc. New York, (1985).

16. J.M. Thomas and W.J. Thomas, *"Introduction to the Principles of Heterogeneous Catalysis"*, Academic Press Inc., New York, (1975), 16.

CHAPTER THREE

THE CHARACTERISATION OF COPPER BASED CATALYSTS BY SELECTIVE CHEMISORPTION

3.1 INTRODUCTION

The electronic structure of a catalyst determines if it is suitable for particular chemical reactions, but it is the surface area of the solid catalysts that determines its effectiveness. A knowledge of the accessibility of the active catalyst surface to reacting gases is not only of considerable importance because it is often closely related to catalyst activity, but also for catalyst development and the study of sintering and poisoning (1).

As supported copper catalysts are of immense industrial importance (see Chapter 1, Section 1.4), it is not surprising that many chemisorption techniques and adsorbate gases ("probe molecules") have been used in an attempt to estimate the exposed copper metal surface area. Carbon monoxide chemisorption has been used at ambient conditions (2), but due to the low heat of adsorption, it is difficult to differentiate between physically and chemically adsorbed gas. Thus the difference between the total CO adsorption isotherm and a physical adsorption isotherm of nitrogen must be used to determine total monolayer coverage. In catalysts where the metallic surface area is small compared to the total surface area, this difference becomes impossible to determine because the physical isotherm lies very close to the isotherm representing the total amount of adsorbed carbon monoxide. The problem is further compounded because of unknown CO/Cu_s stoichiometry. Scholten et al. (3) concluded that hydrogen was not a good choice for gas adsorption onto copper because of plane specificity characteristics and a low degree of metal coverage at ambient temperature and pressure. His findings were based on extensive work by Pritchard *et al.* (4) who

proved that the low index faces of copper, namely (100), (110) and (111) were inactive at ambient temperature. Oxygen is readily chemisorbed onto copper in a complex and temperature dependant interaction which often results in partial and slow oxidation of the bulk material (2). Nevertheless, Parris and Klier (5) showed that under carefully controlled conditions, reliable surface area results could be achieved by O_2 adsorption.

The method of adsorptive decomposition of nitrous oxide has provided an alternative approach to oxygen chemisorption for determining the metal surface areas of both pure and supported copper catalysts (6). The reaction of nitrous oxide with copper surfaces was studied by Dell *et al.* (7) who observed that firstly, only oxygen is taken up by copper and secondly, that decomposition of one nitrous oxide molecule corresponded to the formation of only one nitrogen molecule, resulting in no pressure change during the reaction:

$$N_2O(g) \rightarrow O_{(ads)} + N_2(g) \qquad - (3.1)$$

The lower reactivity of both surface and bulk copper with nitrous oxide as compared to the reactions with oxygen are considered by Scholten *et al.* (3) to be related to the difference in electronic structure between the two molecules. The linear nitrous oxide molecule is stabilized by resonance, whereas oxygen is the more reactive, owing to its 'pseudo-radical' character, caused by the presence of two unpaired electrons in different p-levels. Thus, the kinetics of the reaction with nitrous oxide is more ideal for copper surface area determination because greater control between bulk and surface oxidation is possible. From Figure 3.1 the point of oxygen breakthrough (oxidation of subsurface layers) can be clearly identified at temperatures of 120°C and 140°C.

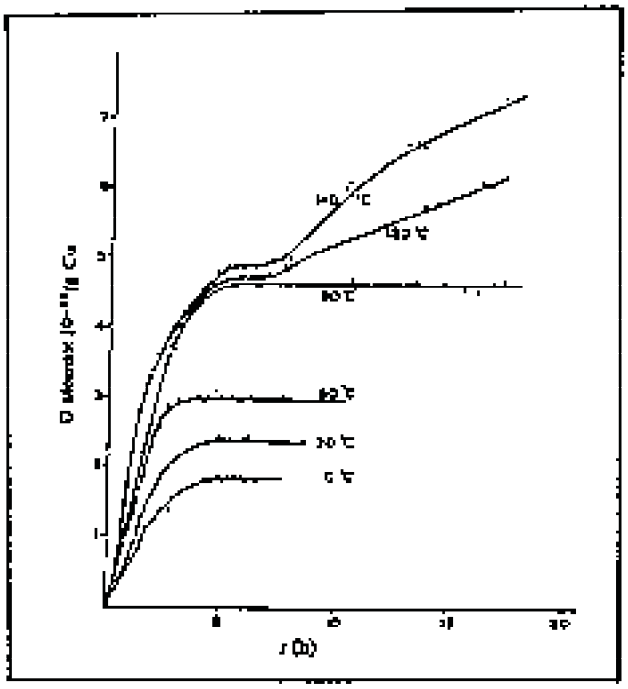

Figure 3.1 Oxygen chemisorption via nitrous oxide decomposition on a copper-on-MgO catalyst at various temperatures as a function of time of contact with N_2O (1)

Mechanistically, it has been considered (7) that the nitrous oxide molecule is adsorbed onto the surface of a copper particle prior to decomposition into a nitrogen and an adsorbed oxygen ion. Nitrogen is subsequently desorbed.

Dell *et al.* (7) measured the reaction enthalpy for various values of oxygen coverage and found them to be equal to half the heat of chemisorption of oxygen plus the enthalpy of decomposition of nitrous oxide. From the thermodynamic correspondence between the two surface reactions, they concluded that the oxygen atoms from nitrous oxide and from oxygen are adsorbed on the same sites and in the same form.

The same authors also established a surface stoichiometry of $Cu_{(s)}/O_{ads} = 2$ at approximately 25% surface coverage by oxygen and a temperature of 20°C. This ratio was confirmed by Scholten and Konvalinka (1) who showed better reproducibility around 90 - 100°C with almost full surface

coverage by oxygen. Thus, the complete reaction of nitrous oxide with copper may be represented according to Equation 3.2.

$$N_2O(g) + 2Cu_s \rightarrow (Cu_s)_2O + N_2(g) \qquad - (3.2)$$

where: S = surface atoms

The quantity of nitrogen formed by the decomposition of the nitrous oxide gives a means of direct measurement of the metallic copper surface area.

There is no agreement in the literature as to the optimum temperature at which the reaction should be performed. Evans *et al.* (8) reported data which is in agreement with a reaction temperature of 90 - 100°C as reported by Scholten and Konvalinka (1), and indicated that bulk oxidation occurs from a temperature of approximately 120°C. Sengupta *et al.* (9) state that a sharp increase in N_2O decomposition at 70°C may be interpreted as the onset of bulk oxidation. They also consider that bulk oxidation starts as low as 67°C, whilst Chinchen *et al.* (6) recommend an operating temperature of 60°C, which is in accordance with the result of many researchers who concluded that no substantial change in the uptake of N_2O occurs between 20 and 80°C. Also, Osinga *et al.* (10) recommend measurements be carried out at temperatures of 20 - 120°C as bulk oxidation is only apparent from 150°C.

A variety of experimental techniques have been used to determine the extent of the reaction of N_2O with the copper surface. Early experiments by Dell *et al.* (7) and Osinga *et al.* (10) employed a *static system* which involved freezing out unreacted N_2O and measuring the residual nitrogen pressure in a volumetric adsorption apparatus. Scholten and Konvalinka (1) used a high vacuum apparatus which permitted alternate circulation of N_2O over the

catalysts at constant temperature and pressure. After required time intervals small gas samples were withdrawn from the system and analysed by thermal conductivity and mass spectroscopy. Giamello *et al.* (11) used microcalorimetry to follow the interaction of N_2O with copper. A microcalorimeter was connected to a volumetric apparatus which enabled the dosing of small amounts of N_2O onto a catalyst. Various forms of pulsed chromatographic methods have been tested. For example, Dvořák and Pašek (12) injected pulses of N_2O into a helium carrier stream as it passed over a sample of catalyst. The excess nitrous oxide from reaction was removed from the $He-N_2$ gas mixture by cooling in liquid nitrogen, or by irreversible adsorption on an activated molecular sieve at 20°C. Nitrogen released during the reaction was analysed by thermal conductivity.

Evans *et al.* (8) further refined this method by using a thermistor element of a thermal conductivity detector to analyse gas mixtures directly. Their apparatus also permitted *in situ* BET determination of samples. Chinchen *et al.* (6) developed a flow chromatographic method by exposing the sample to a dilute mixture of N_2O in helium. A mass spectrometer and katharometer were used for gas detection.

Bond and Namijo (2) have recently used TPR to directly determine the number of oxygen atoms chemisorbed by reaction of N_2O with reduced copper catalysts. This was done in an attempt to firstly minimize the disadvantages encountered when measuring very low N_2 pressures in the volumetric method and secondly, to avoid the reported difficulty of identifying conditions giving complete reaction but no bulk oxidation when utilising the pulse technique.

In this study an attempt has been made to demonstrate that a pulse chromatographic technique may be used to obtain reliable and comparable results. Optimisation of the

technique involved considering the following aspects:

(i) Copper surface atomic density (Cu atoms.m^{-2}). The copper surface areas are calculated on the basis of a knowledge of the copper surface atomic density. Disagreement over the value to be used is evident in the literature. Osinga *et al.* (10) and Dvořák and Pašek (12) calculated a value of 1.36×10^{19} Cu atoms.m^{-2} on the assumption that the (100), (110) and (111) planes are equally present on the surface. Using the same assumption, Dell *et al.* (7) calculated 1.46×10^{19} Cu atoms.m^{-2} based on a value of 6.8 $Å^2$ for the mean area per copper site, as compared to 7.41 $Å^2$ used by Osinga *et al.* (10) and Dvořák and Pašek (12). Scholten and Konvalinka (1) calculated a value of 1.7×10^{19} Cu atoms.m^{-2} on the basis of an equilibrium surface plane distribution in copper of 25% of (100) planes, 5% of (110) planes and 70% of (111) planes. The plane distribution reported by Sundquist (14) gives an average site density of 1.68×10^{19} Cu atoms.m^{-2}.

(ii) Volume and number of nitrous oxide pulses. Evans *et al.* (8) recommended a single pulse of 3 to 4 times greater volume than that decomposed is necessary to eliminate kinetic effects associated with Reaction 3.2, whilst Koeppel *et al.* (13) injected a number of pulses of a standard 0.5 cm^3 volume.

(iii) Mass of sample.

(iv) Temperature of reaction and the identification of surface and bulk oxidation.

(v) Suitability of the method for determining the copper surface area of Raney and co-precipitated catalysts. CO back titration was employed to determine the accuracy of the pulse technique. This involved reducing the copper surface (oxidised by the decomposition of nitrous oxide) with carbon monoxide, to form CO_2 gas according to Equation 3.3.

$$CO(g) + (Cu_s)_2O \rightarrow CO_2(g) + 2Cu \qquad - (3.3)$$

By quantifying the CO_2 formed during reduction, the copper surface area could be estimated.

(vi) Evaluation of the effect of supports with regard to the adsorptive decomposition of nitrous oxide. Scholten *et al.* (3), for example, reported that commercial silicones may show some N_2O decomposition activity, whilst Evans *et al.* (8) found that copper catalysts containing oxides of chromium, zinc and aluminium promoted bulk oxidation.

For all calculations, the surface oxygen coverage, θ, is defined according to the definition of Scholten and Konvalinka such that $\theta = 1$ for $Cu_s/O_{ads} = 2$

where:

$$\theta = \frac{S_{Cu}}{S_{BET}} \qquad - (3.4)$$

and S = surface area ($m^2.g^{-1}$)

3.2 EXPERIMENTAL

3.2.1 Apparatus

The atmospheric pressure flow system was designed to determine copper surface areas by pulse chemisorption and total surface area of the reduced (or oxidised) samples by the single point BET method. The apparatus is similar to the design employed by Evans *et al.* (8) and is shown in Figure 3.2.

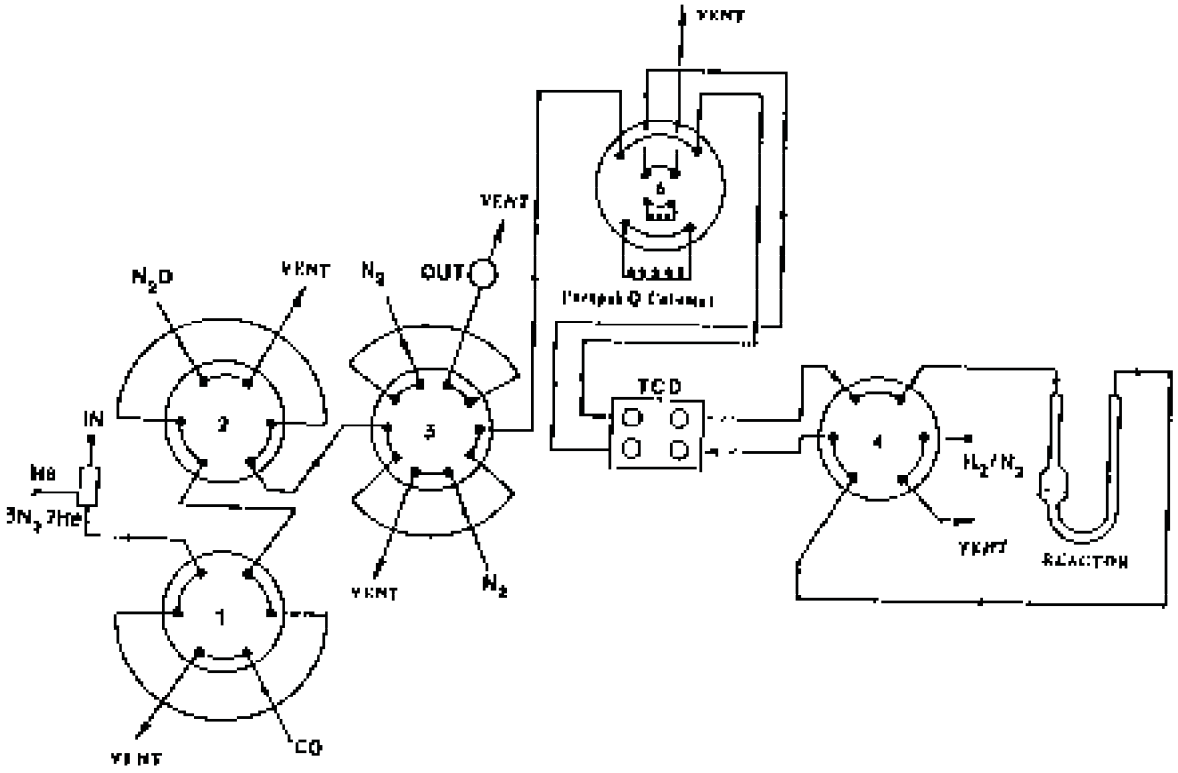

Figure 3.2 Schematic diagram of the pulse chemisorption apparatus, configured for BET determination (modified from reference 8)

A modified Varian 3300 gas chromatograph with a thermal conductivity detector was linked to a Spectra Physics SP4270 integrator, and used for gas analysis. Helium carrier gas (99.999% purity, FEDGAS) or a mixed carrier gas of composition 27.3% nitrogen in helium (FEDGAS) could be selectively brought on line as required by means of the three-way valve as graphically portrayed in Figure 3.2. Both carrier gases and nitrous oxide (99.999% purity, FEDGAS) were further purified by means of oxisorbs (guaranteed final purity of < 0.1 ppm O_2 and < 0.5 ppm H_2O and CO_2 contaminants. Nitrogen (99.999% purity, FEDGAS) and the 5% hydrogen in nitrogen gas mixture (FEDGAS) were not further purified. Flow rates were controlled using Whitey fine flow control needle valves and flow indicators (Aalburg Instruments and Control Inc., USA 0 - 2 l gas/h).

Three Valco six port valves and one ten port Valco valve (all pneumatically controlled by solenoid valves) were mounted externally on the gas chromatograph, and are labelled 1 - 4 in Figure 3.2. One eight port Valco valve (valve No. 5) was positioned in the gas chromatograph oven to provide a manual means of isolating the two stainless steel 1.5m 1/8" Porapak Q columns (Supelco, USA). The five Valco valves formed the framework of the apparatus. The sample was placed on the sintered frit of a reactor chamber positioned midway along an upright arm of the Pyrex U-shaped tube (of 1/4" OD). The modified U-tube was of singular construction thus restricting sample access to the top opening of the upright arm. An all glass external thermocouple well extended to just above the sintered frit of the reactor chamber, providing a means of maintaining sample temperature via a Type J thermocouple probe linked to a digital readout (Rex-C1, RKC Instruments). An interchangeable PID (Rex P9) temperature controlled oven/Dewar flask could be manoeuvred into position by a pneumatically controlled cylinder without moving the sample U-tube, thus enabling both BET and pulse chemisorption measurements without sample transfer.

3.2.2 Samples

Raney catalysts were prepared according to the method reported in Chapter 2, Section 2.1.1 by base leaching alloys B, C and D to achieve final respective atomic compositions of (i) Cu(61.7) Zn(11.0) Aℓ(25.9), (ii) Cu(60.2) Zn(4.2) Aℓ(31.3) and (iii) Cu(70.2) Aℓ(29.8).

A co-precipitated catalyst and commercial ICI 53/1 catalyst of Cu:Zn:Aℓ atomic ratio 1:2.5:3 and 1:1.2:1.6 respectively were also tested. All catalyst compositions were determined by AAS using the technique reported in Chapter 2, Section 2.5. A copper powder was prepared from $Cu_2(OH)_2CO_3$ (Merck analytical reagent grade) by calcination (in a muffle furnace at 300°C for 16.0 hours and *in-situ* reduction (see Section 3.2.3)).

3.2.3 Sample activation

For both the chemisorption (copper surface area) and physisorption ("single point" BET surface area) experiments, each sample was reduced in a 5% hydrogen in nitrogen gas mixture (FEDGAS) at a flow rate of 30ml/min. Before sample activation commenced, valve No. 4 was switched to a position which isolated the sample U-tube from the main apparatus, but simultaneously permitted the reducing gas to flow past the sample. Figure 3.3 shows the correct valve position for activation.

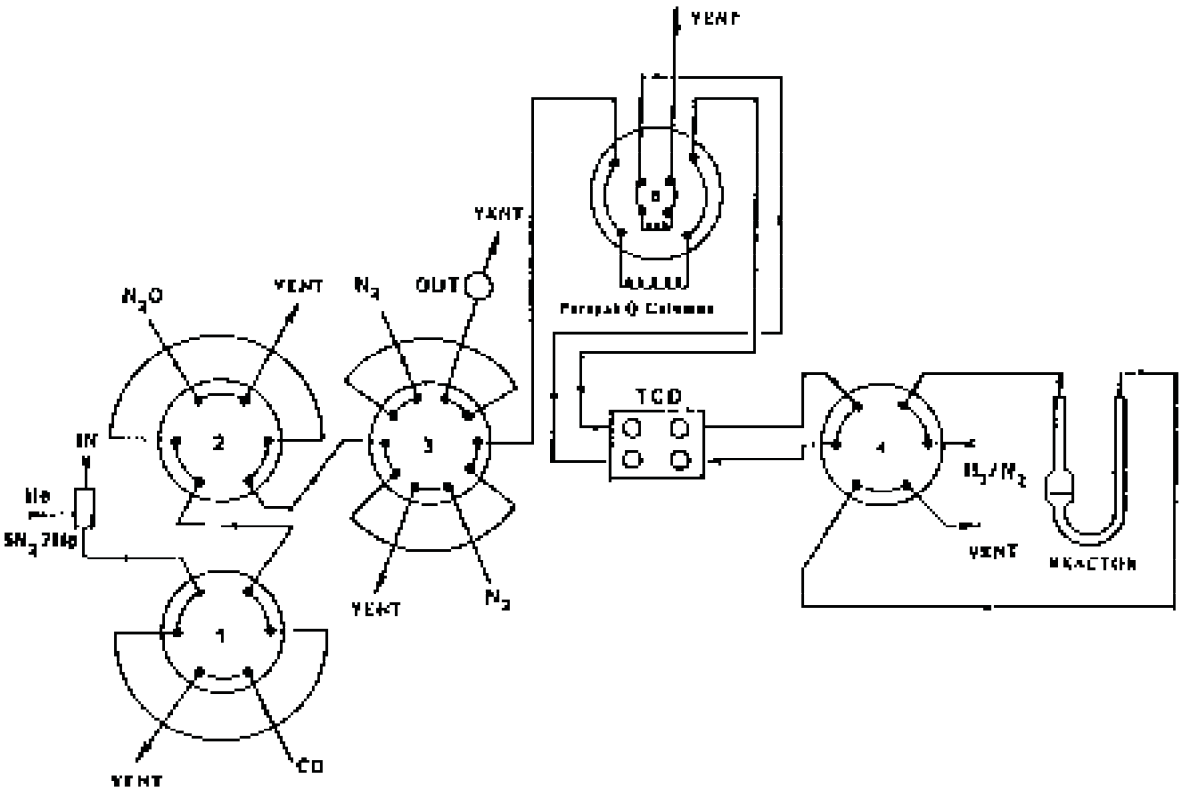

Figure 3.3 Schematic diagram of the pulse chemisorption apparatus, configured for sample activation (modified from reference 8)

In order to minimize sintering, a temperature ramp rate of 30°C/h to a maximum of 230°C for 5 hours was adopted. At the end of the reduction period carrier gas was substituted for the hydrogen mixture (by reversing valve No. 5's position), thus enabling hydrogen to be flushed from the system before commencing with surface area determinations.